A Proteomic Investigation of Ligand-dependent HSP90 Complexes Reveals CHORDC1 as a Novel ADP-dependent HSP90-interacting Protein*[S]

Jacob J. Gano‡ and Julian A. Simon‡§¶

Structural studies of the chaperone HSP90 have revealed that nucleotide and drug ligands induce several distinct conformational states; however, little is known how these conformations affect interactions with co-chaperones and client proteins. Here we use tandem affinity purification and LC-MS/MS to investigate the proteome-wide effects of ATP, ADP, and geldanamycin on the constituents of the human HSP90 interactome. We identified 52 known and novel components of HSP90 complexes that are regulated by these ligands, including several co-chaperones. Interestingly, our results also show that geldanamycin treatment causes HSP90 complexes to become significantly enriched for core transcription machinery, suggesting that HSP90 inhibition may have broad based effects on transcription and RNA processing. We further characterized a novel ADP-dependent HSP90 interaction with the cysteine- and histidine-rich domain (CHORD)-containing protein CHORDC1. We show that this interaction is stimulated by high ADP:ATP ratios in cell lysates and *in vitro* with purified recombinant proteins. Furthermore, we demonstrate that this interaction is dependent upon the ability of HSP90 to bind nucleotides and requires the presence of a linker region between the CHORD domains in CHORDC1. Together these findings suggest that the HSP90 interactome is dynamic with respect to nucleotide and drug ligands and that pharmacological inhibition of HSP90 may stimulate the formation of specific complexes. ***Molecular & Cellular Proteomics 9:255–270, 2010.***

The dimeric HSP90 ATPase is a highly abundant molecular chaperone that functions in later stages of protein folding pathways to assist the folding and activation of a specific set of proteins known as "clients." The essential functions of HSP90 are underscored by the growing list of client proteins functioning in diverse biological processes such as cell division, metabolism, signal transduction, transcription, and immunity. Pharmacological inhibition of HSP90 ATPase activity is generally believed to cause proteolytic degradation of the client protein, leading to alteration of the associated biological processes. HSP90 has become an important target for anticancer therapies because of its role in stabilizing proteins directly involved in oncogenic pathways (1). Consequently, intensive efforts have been put forth to develop HSP90 inhibitors.

HSP90 complexes contain several co-chaperones and accessory proteins that modulate ATPase activity and client protein interactions (2). It is believed that these co-chaperone interactions may direct HSP90 activity to particular complexes and structures within the cell, thereby introducing a degree of selectivity for particular subsets of client proteins (3). It has also been proposed that the binding of co-chaperones can physically alter the client protein binding surfaces on HSP90, thus restricting chaperone activity to a discrete subset of client protein substrates (4, 5). For example, the co-chaperone CDC37 is found almost exclusively in HSP90 complexes containing kinase client proteins and may therefore serve as a kinase-specific adaptor (6).

There is increasing evidence that constituents of HSP90 complexes are influenced by the ligand-bound state of HSP90 (7, 8). The co-chaperone AHSA1 binds exclusively to the ATP-bound HSP90 and stimulates ATP hydrolysis, and this interaction is thought to influence client protein activation (9–12). In addition, several studies have shown the co-chaperone p23 to preferentially interact with the ATP-bound HSP90, inhibiting ATP hydrolysis (7, 13–15). Inhibition of ATP binding and hydrolysis by the pharmacological inhibitor geldanamycin is generally observed to disrupt HSP90 interactions with co-chaperones and client proteins; however, some exceptions exist where geldanamycin has no effect or stabilizes interactions (16, 17). Less is understood about how ADP binding affects HSP90 interactions. Crystallographic evidence from the *Escherichia coli* HSP90 homolog HtpG suggests that the ADP-bound HSP90 adopts a conformation distinct from the ATP-bound form, and it was proposed that this conformation may alter the constituents of HSP90 complexes (18–20).

Several groups have recently reported proteomics studies of the HSP90 interactome; however, these studies were focused on documenting HSP90 interactions under single

From the ‡Clinical Research Division and §Human Biology Division, Fred Hutchinson Cancer Research Center, Seattle, Washington 98109

Received, June 8, 2009, and in revised form, September 21, 2009
Published, MCP Papers in Press, October 28, 2009, DOI 10.1074/mcp.M900261-MCP200

experimental conditions with isolated proteins or were not designed to study how the dynamic interactions of this chaperone complex are influenced by HSP90 ligands (21–27). To gain proteome-wide resolution on the effects of ligands on the HSP90 interactome, we affinity-purified human HSP90 complexes from HEK293T cells in the presence of excess ATP, ADP, or the HSP90 inhibitor geldanamycin and used LC-MS/MS and spectral counting to quantify the effects of these ligands on the constituents of the HSP90 interactome.

EXPERIMENTAL PROCEDURES

Plasmids—Expression vectors for proteomics analysis were derived from the parental TAP[1] expression vector pGlue (28). The TAP tag contains a strep tag peptide sequence that binds streptavidin with high affinity, an intervening tobacco etch virus protease cleavage sequence, and a calmodulin-binding peptide. Full-length human HSP90AA1 (HSP90α) cDNA was constructed by fusing the 5′ end (GenBank™ accession number BQ276361.1) and the 3′ end (GenBank accession number BC023006.1) using GenBank accession number X15183 as a reference sequence. N-terminal TAP fusions of the wild type HSP90α and mutants were created by site-directed mutagenesis and PCR amplification from cDNAs and verified by sequencing. Human CHORDC1 cDNA was constructed from RNA isolated from HEK293T cells and PCR-amplified. Subsequent co-expression analysis was performed using pCS2+ parental vectors for all C-terminal HSP90-TAP constructs and pSPORT6 (Invitrogen) for expression of HA-tagged CHORDC1 constructs in HEK293T cells. For *E. coli* expression vectors, HSP90 and HA-CHORDC1 coding sequences were PCR-amplified from the above vectors and cloned into pGWS (pGEX derivative; kindly provided by Bruce Clurman, Fred Hutchinson Cancer Research Center) and pET16b (Novagen) for N-terminal GST-tagged HSP90 and N-terminal His-tagged HA-CHORDC1 constructs, respectively. All constructs were verified by sequencing.

Cell Culture and Viability Assay—Low passage number HEK293T cells (ATCC CRL-1573) were used in all experiments. Cells were grown in high glucose Dulbecco's modified Eagle's medium containing 10% fetal bovine serum, penicillin, streptomycin, and 2 mM supplemental L-glutamine (Invitrogen). All incubations were at 37 °C with humidified 5% CO_2. HEK293T cells carrying HSP90-TAP constructs used for proteomics analysis were stably selected and maintained using puromycin (Sigma-Aldrich). The ATPlite cell viability assay (PerkinElmer Life Sciences) was used to determine relative growth rates of all clones expressing HSP90 in 96-well plates according to the manufacturer's instructions.

Nucleotide and Geldanamycin Stocks—Stocks of 250 mM ATP were made in 50 mM HEPES, 5 mM $MgCl_2$ (pH 8.0) and treated with 50 mM phosphocreatine and 50 μg/ml creatine kinase (Roche Applied Science) for 3 h at 20 °C. Stocks of ADP were made in 50 mM HEPES, 5 mM $MgCl_2$ (pH 8.0) with 100 mM glucose and 20 units/ml hexokinase (Roche Applied Science) and incubated for 3 h at 20 °C. Both stocks were then subjected to ultrafiltration at 4 °C using YM-3 (3,000-Da cutoff) filters (Millipore, Billerica, MA) to remove enzymatic activity. 20 mM geldanamycin stock (NCI, Bethesda, MD) was prepared in 100% DMSO.

Tandem Affinity Purification and Mass Spectrometry—Purifications for all experimental groups, including the vector control, were repeated independently in triplicate, and resulting protein complexes were analyzed by MS consecutively. Affinity purifications were adapted from Angers *et al.* (28). 7.5×10^8 HEK293T cells were grown to 100% confluence on 15-cm coated plates (catalog number 168381, Nunc, Roskilde, Denmark) without puromycin. Two hours before lysis, the cells were treated with 5 μM geldanamycin in 0.1% DMSO where indicated or left untreated. The cells were gently washed twice with PBS at 4 °C, subsequently detached from the plate by aspiration with PBS, and centrifuged for 2 min at 4 °C in a clinical centrifuge. All further procedures were conducted at 4 °C unless otherwise noted. The supernatant was replaced with 7.5 ml of TAP lysis buffer containing 50 mM HEPES-KOH (pH 8.0), 10% glycerol, 0.1% Nonidet P-40, 150 mM KCL, 5 mM $MgCl_2$, 2 mM DTT, and an EDTA-free protease inhibitor mixture tablet (Roche Applied Science). Before lysis, buffer was supplemented with either 5 mM ATP including an ATP regeneration system (50 mM phosphocreatine and 50 μg/ml creatine kinase) (29), 5 mM ADP with an ATP depletion system (100 mM glucose and 20 units/ml hexokinase), (30), or 5 μM geldanamycin (GA) with 0.1% DMSO. ATP concentrations were monitored throughout the procedure using the Cell Titer-Glo® ATP assay (Promega, Madison, WI). Lysates were cleared by centrifugation, and supernatants were added to 200 μl of packed streptavidin beads (GE Healthcare) that were prewashed three times and equilibrated in 300 μl of TAP lysis buffer. The remaining steps were conducted essentially as reported (31) with the following exceptions: tobacco etch virus protease cleavage was eliminated as free biotin alone eluted most of the bound HSP90; ATP, ADP, and GA were added to all buffers except the elution buffer. Protein complexes were finally eluted from calmodulin beads three times in 300 μl for a total of 900 μl. Each sample was adjusted to 50 mM ammonium bicarbonate, and the disulfide bonds were reduced with 5 mM dithiothreitol for 1 h. The proteins were digested overnight with modified porcine trypsin (V5111, Promega) at 37 °C. The resulting peptide mixtures were concentrated to 100-μl volumes, desalted using C_{18} ZipTips (Millipore), evaporated to dryness, and resuspended in distilled H_2O with 0.1% formic acid.

Each digested protein mixture was analyzed by automated microcapillary LC-MS/MS. A 75-μm-inner diameter PicoFrit silica capillary nanospray emitter (New Objective, Woburn, MA) was slurry-packed with 20 cm of 5-μm C18AQ (100-Å) packing material (Michrom Bioresources, Auburn, CA) using a pressure bomb. The column was placed in line with a guard column created from a 100-μm-inner diameter IntegraFrit column (New Objective) packed with 1.5 cm of 5-μm C18AQ (200-Å) packing material. The column setup was connected in line to an Eksigent 2D nanoLC system (Eksigent Technologies, Dublin, CA) and interfaced to an LTQ-FT ion trap mass spectrometer (ThermoFisher Scientific, San Jose, CA).

The mobile phase for the HPLC separation was 0.1% formic acid in water (Buffer A) and 0.1% formic acid in acetonitrile (Buffer B). The LC-MS/MS experiments consisted of a 100-min HPLC run where the HPLC gradient started at 2% Buffer B for 5 min, ramped to 10% Buffer B over 3 min, and then ramped to 40% Buffer B over 60 min followed by washing between samples at 80% Buffer B for 12 min and re-equilibration at 2% Buffer B for 20 min.

The LTQ-FT mass spectrometer was operated in the data-dependent acquisition mode using the Xcalibur 2.0SR2 software. The experiment consisted of a single full-scan mass spectrum in the FT (400–1800 *m/z*, 100,000 resolution at *m/z* 400) followed by five data-dependent MS/MS scans in the ion trap at 35% normalized collision energy. The mass spectrometer was set to only perform MS/MS on

[1] The abbreviations used are: TAP, tandem affinity purification; CS, CHORD-Sgt1; TPR, tetratricopeptide repeat; SAF, spectral abundance factor; GA, geldanamycin; HA, hemagglutinin; LTQ, linear trap quadrupole; v., version; CPAS, Computational Proteomics Analysis System; IPI, International Protein Index; FDR, false discovery rate; ANOVA, analysis of variance; WT, wild type; VO, vector only; CHORD, cysteine- and histidine-rich domain; N-TAP, N-terminal TAP tag; C-TAP, C-terminal TAP tag.

ions with identifiable charge states of 2+ or 3+. The dynamic exclusion parameters were as follows: repeat count, 1; repeat duration, 30 s; exclusion list, 100 *m/z* values; and exclusion time, 45 s.

Raw Data Analysis and Database Searching—The MS/MS scans from each LC-MS/MS run were converted from the .RAW file format to .mzXML files using the program ReAdW.exe (v. 1.1) with the default parameters. The spectra were matched to peptides using X!Tandem (v. 2007.07.01.2) (32) configured with a pluggable scoring algorithm (33) compatible with the PeptideProphet™ inference tools (34) bundled in the Computational Proteomics Analysis System (CPAS) data analysis system (v. 8.2) (35). The following parameters were used in the database search: full trypsin enzyme specificity; missed cleavages allowed, 2; peptide mass tolerance, 2.0 Da; fragment ion tolerance, 0.5 Da; monoisotopic molecular weight for both peptide and fragment ion masses; b/y ion search; and variable modification at Met (+15.995), Gln (−17.027) only if on the peptide N terminus, and Glu (−18.011) only if on the N terminus.

The MS/MS spectra were searched against a custom database created by combining the IPI human database (v. 3.52, released November 2008) with a pseudo-reversed version of each protein sequence for the purpose of estimating the false discovery rates (FDRs). The pseudo-reversed sequences were created by identifying all the tryptic protein cleavage sites and holding all terminal lysine and arginine residues static while reversing all other amino acids present within the internal peptide sequences of the protein. The .mzXML peak lists were filtered by X!Tandem during the database search with the following parameters: maximum charge state, 4+; minimum peptide mass, 600 Da; maximum peptide mass, 4000 Da; and minimum number of allowed fragment peaks, 6. The MS/MS database search results were then analyzed using PeptideProphet and ProteinProphet (v. 3.0, April 1, 2004 (TPP v. 2.9 GALE revision 9, Build 200703221424)) both under default settings for peptide and protein identification scoring, respectively. The final results were then organized in CPAS.

Comparison, Normalization, Protein List Filtering, and Statistical Analysis—Peptide and protein scores were generated using PeptideProphet and ProteinProphet software (30, 32). Spectral counting was used to quantify protein abundances, and the following filtering protocol was used to eliminate proteins from additional analysis. Peptide spectra counts for each protein were calculated by CPAS as the total number of individual spectra (unique or non-unique sequences) matched to a protein using ProteinProphet in which the PeptideProphet scores for individual spectra exceeded a 5% FDR. Therefore, the cutoff scores for accepting individual spectra were different for each of the 33 individual MS runs. The FDR was estimated using a target-decoy strategy developed by Gygi and co-worker (36) by searching all spectra against a combined pseudo-reversed and forward IPI database (for details see above). Proteins having less than a 5-fold average spectral abundance over the vector control were considered to be contaminants and were eliminated. Only proteins with four or more spectra total and at least one peptide in each replicate (prenormalization) were allowed. A protein was considered to be identified if it passed these criteria for at least one experimental group. The total spectra count for all proteins from each run was then determined individually and used to normalize all runs. Then all N-TAP runs and C-TAP runs were normalized separately to the spectra counts for HSP90α (HSP90AA1). The spectral abundance factor (SAF) was then determined by dividing the normalized spectra count for an individual protein by the length of the protein in amino acids (37, 38). This calculation accounts for the fact that longer proteins contain more tryptic sites than shorter proteins and forms a basis for determining relative protein abundance. Finally, the list was then searched for common contaminants such as keratin and cytoskeletal components, and these proteins were eliminated.

Redundancy was then analyzed using ProteinProphet where a peptide is matched either to a single protein or to a group of protein sequences sharing that peptide sequence. A probability score was then assigned by the software to reflect the likelihood that a set of peptides originated from a particular protein in the group. ProteinProphet scores for all protein identifications are shown in supplemental Table S3. All proteins reported in this study exceeded a ProteinProphet score of >0.9 in at least one run. One protein group containing HSP70 isoforms is reported where no distinction between these proteins could be made. These proteins were treated as a single group. In cases of bioinformatic redundancy where duplicate or truncated versions of the same protein were included in a protein group along with the full-length protein, the duplicated sequences were eliminated, and spectra counts were reported for only one full-length protein for purposes of calculating the SAF. Where several splicing variants were identified, results were simplified by reporting the spectra counts and calculating the SAF for the isoform with the longest amino acid sequence. The SAFs for the resulting list of interacting proteins were then subjected to ANOVA to determine whether variances were due to any particular experimental condition, and the threshold was set at $p = 0.01$. A post hoc pairwise *t* test determined *p* values for all experimental conditions among N-TAP and C-TAP constructs separately. All computations were performed using R statistical analysis software.

Transfections, Affinity Precipitations, and Western Blotting—1.3×10^6 HEK293T cells were plated in 60-cm plates 24 h before transfection by calcium phosphate precipitation. The medium was changed 18 h post-transfection, and cells were allowed to recover 24 h before lysis. Drug treatments were as described above. Lysates were prepared in 500 μl of TAP lysis buffer, cleared by centrifugation, incubated with 5 μl of streptavidin beads for 5 h in a 1.5-ml deep well 96-well plate, and transferred to an Orochem OF1100 fritted 96-well plate for washing. The bead solution was centrifuged briefly to remove supernatant, washed four times by centrifugation with 250 μl of TAP lysis buffer containing the appropriate nucleotide or drug, and eluted with 20 μl of hot 1.2× SDS-PAGE loading buffer. Western blotting was performed using anti-HA (catalog number MMS-101R, Covance, Emeryville, CA), horseradish peroxidase-conjugated streptavidin (GE Healthcare), or anti-HSP90α (catalog number V10051, Biomedia). ImageJ was used to collect all densitometry data.

Recombinant Protein Expression, Purification, and in Vitro Binding Assays—C-terminal GST-tagged HSP90 and HA-CHORDC1 were expressed in BL21 codon plus *E. coli* (Stratagene, La Jolla, CA) by induction with 0.5 mM isopropyl 1-thio-β-D-galactopyranoside for 4 h at 37 °C. Cells were lysed in TAP lysis buffer (see "Tandem Affinity Purification and Mass Spectrometry" above) using pulsed sonication. HSP90-GST supernatants were incubated with GST beads for 4 h, washed extensively, and stored at −20 °C. His-tagged HA-CHORDC1 supernatants were applied to nickel-nitrilotriacetic acid resin, purified using standard techniques, and stored at −20 °C. All proteins were purified to >80% purity as determined by Coomassie staining. 1 μg of HSP90-GST was incubated with 100 ng of His-tagged HA-CHORDC1 for 5 h in the presence of 5 mM ATP or ADP or TAP lysis buffer alone at 4 °C. Washes and blotting were as described above for affinity precipitations.

Real Time RT-PCR—Total RNA was isolated from HEK293T cells expressing N-terminal TAP-tagged HSP90 either treated for 2 h with 5 μM geldanamycin or DMSO alone. 900 ng of total RNA was subjected to RT using an Affinity Script cDNA synthesis kit (Stratagene) according to the manufacturer's instructions using oligo(dT) primers. An amount equivalent to 20 ng of total RNA was used in real time PCRs using Brilliant II Fast SYBR® Green (Stratagene). All conditions were according to the manufacturer's instructions. PCRs commenced in an ABI 7900HT thermocycler. Primer sequences are avail-


a.
N-Terminal TAP-HSP90
*HSP90AA1
*HSP90AB1
STIP1
HSPA8
FKBP5
CDC37
STUB1
FKBP4
*MYLK2
CHORDC1
TOMM34
PPP5C
SUGT1
CCDC117
AHSA1
*TTC9C
*TTC4
NUDC
BAG2
NUDCD3
PTGES3
ST13
CSNK1A1
POLR2E
*DNAJC7
PLCE1
UNC45A
RPAP3
FAM83H
CDC2L2
ASCC3L1
PIH1D1
*PPP2R1A
c10orf137
c19orf2
CACYBP
EFTUD2
MAP3K7IP1
MAP3K7IP2
LRRIQ2
USP19
CNOT6
SAF
PRPF8
MLF2
CHUK
CDC37L1
IKBKG
DYNC1H1
SCRIB
C22orf30
*FLII
YTHDC2
NR3C1
*CALD1
b.
C-Terminal HSP90-TAP
*HSP90AA1
*HSP90AB1
*MYLK2
SUGT1
CDC37
CALD1
IKBKG
AHSA1
HSPA1A
PPP5C
NUDC
UNC45A
*CACYBP
*FKBP5
CHORDC1
SCRIB
*STIP1
*BAG2
*FAM83H
CHUK
*USP19
*LRRIQ2
SAF
NW/CW ATP
NW/CW ADP
NE/CE ATP
NW/CW GA
* ANOVA p>0.01

able in supplemental Table S9. All reactions were analyzed for multiple products using melting curve analysis. Data were analyzed by REST software (Corbett Lifescience) using β-actin as a reference gene.

RESULTS

Identification of Novel HSP90 Interactions and Those Influenced by Nucleotides and Pharmacological Inhibition—N- and C-terminal TAP-tagged human HSP90α cDNAs were stably expressed in the human kidney epithelial cell line HEK293T, and TAP was performed on HSP90 complexes in the presence of 5 mM ATP, 5 mM ADP, or 5 μM GA. In addition to the wild type HSP90α, we chose to use the E47A mutant that is unable to hydrolyze ATP yet able to bind the nucleotide with affinities comparable to the wild type protein (15, 17, 39). This mutant has been shown to strengthen interactions between HSP90 and substrate peptides *in vitro* and is predicted to function as a kinetic trap to detect interactions with client proteins and co-chaperones *in vivo*. Indeed, the analogous mutation in yeast was previously shown to strengthen the interaction between the yeast p23 homolog Sba1p and the yeast HSP90, an interaction known to be positively influenced by ATP (40). Therefore, HSP90 E47A is predicted to serve as a suitable probe in this system to identify HSP90 interactions that are stabilized by excess ATP. TAPs were performed in three independent replicate experiments containing the following four experimental groups for both N- and C-terminal constructs: 1) wild type HSP90 with ATP (NW ATP and CW ATP), 2) ADP (NW ADP and CW ADP), 3) geldanamycin (NW GA and CW GA), and 4) HSP90 E47A mutant with ATP (NE ATP and CE ATP). An empty vector control with ATP (VO ATP) was included to control for nonspecific binding. Relative quantities of the TAP-tagged proteins were determined by Western blot, and N- and C-terminal constructs were shown to have comparable expression levels (supplemental Fig. S1). All stably expressed constructs were tested for altered growth rates using an ATP assay, and no differences between clones were observed, suggesting that the essential functions of endogenous HSP90 complexes are largely undisturbed by exogenous expression of TAP-tagged HSP90 mutants (supplemental Fig. S2). An ATP regeneration or depletion system was used for all purifications containing ATP or ADP, respectively (see "Experimental Procedures"). For the WT GA group, cells were pretreated with drug for 2 h before harvesting. Purified complexes were then consecutively subjected to LC-MS/MS, and the resulting raw spectra were analyzed using spectral counting and filtered. Spectra counts for all proteins were converted to SAFs to gain a relative measure of the protein abundance among interacting proteins (37, 41). The SAFs were compared across experimental groups, and the average SAFs for identified proteins are presented in Fig. 1. All N-terminal constructs and treatments were compared independently from C-terminal constructs to account for the fact that N-terminal constructs captured about 5-fold more HSP90 than C-terminal constructs. A complete record of raw spectra counts, error analysis, protein and peptide certainty values, and other statistics for each identified protein are found in supplemental Table S3. Spectra and PeptideProphet (certainty) scores for all single peptide identifications are shown in supplemental Fig. S4 and supplemental Table S5. For presentation purposes, all IPI accession numbers for the final table of interacting proteins were converted to the corresponding NCBI protein name.

Identification of Known and Novel HSP90 Interactions—We identified 37 known HSP90-interacting proteins and 24 putative novel interactions (Table I). Of the known interactors, we identified 20 co-chaperones, including seven containing the TPR domain, an established HSP90 interaction element. We also identified a group containing eight HSP70 family members. We were unable to clearly differentiate between HSP70 family members using MS, so these proteins were treated as a single group, and HSPA8 was chosen to represent this group because of its high spectral abundance. All HSP70 family members identified bound HSP90 in a similar manner with respect to ligands (see Table I and supplemental Fig. S6 for data on all HSP70s). Furthermore, we identified seven CHORD-Sgt1 (CS) domain-containing proteins believed to function as co-chaperones, including SUGT1, PTEGS3 (p23), NUDC, CACYBP (SIP), CHORDC1, NUDCD3, and USP19 (23, 42–44). USP19 and NUDCD3 are predicted to form interactions with HSP90 based upon homology to p23 and SUGT1 (45); however, to our knowledge these two interactions have not been previously reported. These findings provide further support for the CS domain as a *bone fide* HSP90 interaction domain. The C-terminal TAP-tagged HSP90 constructs identified considerably fewer proteins with lower spectra counts than the N-terminal TAP constructs, and none of the identifications were unique to the C-terminal constructs. This is most likely because of a relatively lower recovery of C-terminal tagged HSP90 in our purifications as both the N- and C-terminal constructs are expressed at comparable levels (see supplemental Fig. S1). Overall, the identification of many known HSP90-interacting proteins in this data set supports the possibility that we have also identified novel HSP90 interactions.

FIG. 1. **Spectral abundance factors for HSP90-interacting proteins.** *a*, N-terminal TAP-tagged HSP90 interactors. Data are averages of three replicate experiments. Experimental groups are color-coded: WT ATP (*red*), WT ADP (*blue*), E47A ATP (*green*), and WT GA (*yellow*). Proteins are arranged in descending order according to their spectral abundance factor. The *horizontal axis* displays the SAF, and the scales change for every block of proteins to account for the wide range of SAF values for this data set. Protein names are shown to the left. Statistical information including standard deviation is available in supplemental Table S1. *Asterisks* denote proteins that are not regulated by ligands (ANOVA $p > 0.01$) *b*, C-terminal TAP-tagged HSP90 interactors.

TABLE I

Known and novel HSP90-interacting proteins for which HSP90 binding interactions are regulated by ATP, ADP, or geldanamycin

Entrez protein name and GeneID, gene ontology (GO) terms for biological function, and the known functional associations with HSP90 are presented for all identified proteins. ANOVA *p* values and the group in which the protein is overrepresented are listed along with pairwise *t* test confidence intervals. 0, not overrepresented; ER, endoplasmic reticulum.

Entrez protein name	Entrez GeneID	Description	HSP90 interaction type	Biological process (GO)	ANOVA *p* value N/C-TAP HSP90	Overrepresented N/C-TAP
HSP90AA1	3320	HSP90 α	Chaperone, dimeric subunit	Protein folding	4.582*e*−01	0
HSP90AB1	3326	HSP90 β	Chaperone, dimeric subunit	Protein folding	8.02*e*−01/1.33*e*−2	0
STIP1	10963	Stress-induced phosphoprotein 1 (Hsp70/Hsp90-organizing protein; HOP)	TPR domain co-chaperone	Response to stress	9.728*e*−04	0
FKBP5	2289	FK506-binding protein 5 (FKBP54)	TPR domain co-chaperone	Protein folding	7.096*e*−04	0
CDC37	11140	Cell division cycle homolog 37 (CDC37)	Co-chaperone	Protein folding, regulation of CDK activity	2.42*e*−03/4.87*e*−03	0
STUB1	10273	STIP1 homology and U-box-containing protein 1 (CHIP)	TPR domain co-chaperone	Ubiquitination, protein folding	7.798*e*−04	0
MYLK2	85366	Myosin light chain kinase 2, skeletal muscle	Novel interaction	Protein amino acid phosphorylation	3.377*e*−02	0
CCDC117	150275	Coiled coil domain-containing 117	Novel interaction	N/A	8.189*e*−03	0
TTC9C	283237	Tetratricopeptide repeat domain 9C	Novel interaction	N/A	9.419*e*−02	0
TTC4	7268	Tetratricopeptide repeat domain 4	TPR domain-containing	Binding	1.687*e*−01	0
DNAJC7	7266	DnaJ (Hsp40) homolog, subfamily C, member 7 (TPR2)	TPR domain co-chaperone	Protein folding	7.962*e*−02	0
PLCE1	51196	Phospholipase C, ϵ 1	Novel interaction	Ras protein signal transduction	3.955*e*−06	0
CDC2L2	728642	Cell division cycle 2-like 2 (CDK11)	Client	Cell cycle	2.094*e*−07	0
PPP2R1A	5518	Protein phosphatase 2 (formerly 2A), regulatory subunit A, α isoform	Novel interaction	Cell cycle	1.024*e*−02	0
EFTUD2	9343	Elongation factor Tu GTP binding domain-containing 2	Novel interaction	Protein biosynthesis, RNA splicing	3.216*e*−04	0
CNOT6	57472	CCR4-NOT transcription complex, subunit 6	Novel interaction	Regulation of transcription	5.230*e*−04	0
PRPF8	10594	PRP8 pre-mRNA processing factor 8 homolog	Novel interaction	mRNA splicing	3.037*e*−03	0
CHUK	1147	Conserved helix-loop-helix ubiquitous kinase (IKBKA)	Client	Immune response	1.103*e*−03	0
FLII	2314	Flightless 1 homolog	Novel interaction	Regulation of transcription	1.807*e*−02	0
CALD1	800	Caldesmon-1	Novel interaction	Cell motion	4.58*e*−01/1.31*e*−02	CW ATP[a]
PPP5C	5536	Protein phosphatase 5, catalytic subunit	Co-chaperone	Mitosis, transcription	4.78*e*−8/2.78*e*−02	ΔMEEVD GA[b]
USP19	10869	Ubiquitin-specific protease 19	CS domain co-chaperone	Ubiquitination	2.770*e*−05	ΔMEEVD GA[a]
SUGT1	10910	SGT1, suppressor of G2 allele of SKP1	CS domain co-chaperone	Ubiquitination, mitosis	3.09*e*−08/9*e*−04	NE ATP[b]/CE ATP[a]
AHSA1	10598	Activator of heat shock protein ATPase homolog 1 (AHA1)	Co-chaperone	Protein folding, response to stress	2.98*e*−07/3.21*e*−09	NE ATP[b]/CE ATP[b]
NUDC	10726	Nuclear distribution gene C	CS domain co-chaperone	Mitosis	4.89*e*−11/4.5*e*−5	NE ATP[b]/CE ATP[c]
NUDCD3	23386	NudC domain-containing 3	CS domain co-chaperone	N/A	8.923*e*−08	NE ATP[b]
PTGES3	10728	Prostaglandin E synthase 3 (p23)	CS domain co-chaperone	Protein folding, signal transduction	5.545*e*−04	NE ATP[a]

TABLE I—*continued*

Entrez protein name	Entrez GeneID	Description	HSP90 interaction type	Biological process (GO)	ANOVA *p* value N/C-TAP HSP90	Overrepresented N/C-TAP
CSNK1A1	1452	Casein kinase 1, α 1	Novel interaction	Wnt signaling	3.897*e*−09	NE ATP[a]
UNC45A	55898	Unc-45 homolog A (SMAP1)	Co-chaperone	Protein folding, muscle development	9.06*e*−076/1.87*e*−03	NE ATP[b]/CE ATP[a]
FAM83H	286077	Family with sequence similarity 83, member H	Novel interaction	N/A	4.250*e*−10	NE ATP[b]
CACYBP	27101	Calcyclin-binding protein (SIP)	CS domain co-chaperone	Ubiquitination	4.117*e*−10	NE ATP[b]
MAP3K7IP1	10454	Mitogen-activated protein kinase kinase kinase 7-interacting protein 1 (TAK1)	Client	Activation of MAPKKK activity	2.014*e*−04	NE ATP[c]
MAP3K7IP2	23118	Mitogen-activated protein kinase kinase kinase 7-interacting protein 2	Novel interaction	N/A	1.455*e*−05	NE ATP[b]
LRRIQ2	79598	Leucine-rich repeats and IQ motif-containing 2	Novel interaction	N/A	2.025*e*−03	NE ATP[a]
IKBKG	8517	Inhibitor of κ light polypeptide gene enhancer in B-cells, kinase γ (NEMO)	Client	Regulation of transcription	1.521*e*−05	NE ATP[b]/CE ATP[a]
DYNC1H1	1778	Dynein, cytoplasmic 1, heavy chain 1	HSP90 complex transporter	Microtubule-based movement	1.165*e*−03	NE ATP[a]
SCRIB	23513	Scribbled homolog	Novel interaction	Cell polarity	2.65*e*−05/9.45*e*−04	NE ATP[c]/CE ATP[a]
c22orf30	253143	Chromosome 22 open reading frame 30	Novel interaction	N/A	1.534*e*−12	NE ATP[b]
CHORDC1	26973	CHORD-containing 1 (CHP1)	CS domain co-chaperone	N/A	4.55*e*−10/3.21*e*−09	NW ADP[b]
c10orf137	26098	Erythroid differentiation-related factor 1 (EDRF1)	Novel interaction	Regulation of transcription	2.740*e*−04	NW ADP[a]
HSPA8	3312	Heat shock 70-kDa protein 8	Chaperone/co-chaperone	Response to unfolded protein	8.72*e*−05/1.87*e*−06	NW GA[c]/CW GA[b]
FKBP4	2288	FK506-binding protein 4, 59 kDa (FKBP52)	TPR domain co-chaperone	Protein folding	2.058*e*−05	NW GA[c]
TOMM34	10953	Translocase of outer mitochondrial membrane 34	Novel interaction	Protein folding, protein mitochondrial targeting	3.004*e*−06	NW GA[c]
BAG2	9532	BCL2-associated athanogene 2	Co-chaperone	Protein folding, apoptosis,	6.271*e*−03	NW GA[a]
ST13	6767	Suppression of tumorigenicity 13 (colon carcinoma) (Hsp70-interacting protein; HIP)	Co-chaperone	Protein folding	8.790*e*−03	NW GA[a]
POLR2E	5434	Polymerase (RNA) II (DNA-directed) polypeptide E, 25 kDa	Novel interaction	Transcription from RNA polymerase II promoter	7.452*e*−06	NW GA[b]
RPAP3	79657	RNA polymerase II-associated protein 3	Co-chaperone	Transcription	2.073*e*−03	NW GA[a]
ASCC3L1	23020	Activating signal cointegrator 1 complex subunit 3-like 1	Novel interaction	RNA splicing	3.696*e*−05	NW GA[a]
PIH1D1	55011	PIH1 domain-containing 1 (Pih1p, NOP17)	Co-chaperone	Metabolism, preRNA processing	2.655*e*−05	NW GA[c]
c19orf2	8725	Chromosome 19 open reading frame 2 (unconventional prefoldin RPB5 interactor)	Novel interaction	Protein folding, regulation of transcription	2.588*e*−04	NW GA[a]
MLF2	8079	Myeloid leukemia factor 2	Novel interaction	Protein binding, defense response	2.472*e*−07	NW GA[b]
CDC37L1	55664	Cell division cycle 37 homolog (*Saccharomyces cerevisiae*)-like 1	Co-chaperone	Protein binding	2.472*e*−07	NW GA[b]
YTHDC2	64848	YTH domain-containing 2	Novel interaction	Inferred RNA binding/ helicase	3.673*e*−04	NW GA[a]
NR3C1	2908	Nuclear receptor subfamily 3, group C, member 1 (glucocorticoid receptor)	Client	Regulation of transcription	9.738*e*−06	NW GA[b]

TABLE I—*continued*

Entrez protein name	Entrez GeneID	Description	HSP90 interaction type	Biological process (GO)	ANOVA *p* value N/C-TAP HSP90	Overrepresented N/C-TAP
HSPA8	3312	Heat shock 70-kDa protein 8 (HSC70)	Chaperone/co-chaperone	Response to unfolded protein	8.72e−05/1.87e−06	NW GA[c]/CW GA[b]
HSPA7	3311	Heat shock 70-kDa protein 7 (HSP70B)	Chaperone/co-chaperone	Response to unfolded protein	6.075e−03	NW GA[a]
HSPA6	3310	Heat shock 70-kDa protein 6	Chaperone/co-chaperone	Response to unfolded protein	2.623e−04	NW GA[a]
HSPA5	3309	Heat shock 70-kDa protein 5 (Bip)	Chaperone/co-chaperone	ER overload response	7.14e−07/5.82e−04	NW GA[b]/CW GA[a]
HSPA2	3306	Heat shock 70-kDa protein 2	Chaperone/co-chaperone	Response to unfolded protein	2.752e−04	NW GA[c]
HSPA1L	3305	Heat shock 70-kDa protein 1-like	Chaperone/co-chaperone	Response to unfolded protein	4.972e−06	NW GA[b]
HSPA1A	3303	Heat shock 70-kDa protein 1A	Chaperone/co-chaperone	Response to unfolded protein	2.19e−07/1.04e−02	NW GA[b]/CW GA[a]
HSPA9	3313	Heat shock 70-kDa protein 9 (mortalin)	Chaperone/co-chaperone	Response to unfolded protein	1.393e−04	NW GA[c]

[a] Pairwise *t* test *p* value confidence interval: $p < 0.05$.
[b] Pairwise *t* test *p* value confidence interval: $p <= 0.0001$.
[c] Pairwise *t* test *p* value confidence interval: $p < 0.001$.

Our data set also contained five known client proteins. We identified two kinases forming novel HSP90 interactions (CSNK1A1 and MYLK2). The presence of the known HSP90 client kinases CHUK and CDC2L2 (CDK11) taken together with the identification of the kinase-specific co-chaperone CDC37 in our purifications further strengthens the possibility that these kinases may be HSP90 client proteins. However, it must be noted that several known kinase client proteins are absent from our data. The detection of particular client proteins may be dependent upon their expression levels, and some HSP90 clients may be conditionally expressed, cell cycle-dependent, or not expressed in the renal epithelium from which the HEK293T cells were derived.

Identification of Ligand-dependent HSP90 Interactions—It is well established that some interactions with co-chaperones and client proteins are dependent upon the nucleotide- or drug-bound state of HSP90. We sought to identify new ligand-dependent interactions and to observe effects of ligands on the dynamics of the HSP90 interactome. We searched our data set to identify proteins with spectral abundances that were significantly altered in purifications containing one HSP90 ligand over the others. We subjected the SAFs for each protein across experimental groups to ANOVA and identified 52 proteins (including HSP70 homologs) that were below the ANOVA *p* value cutoff of 0.01 (Table I). These proteins represent 84% of the total identifications in this data set, suggesting that HSP90 complexes are sensitive to the ligand present in the purification reactions. We also sought to identify interactions that are specifically formed in the presence of a particular ligand. To this end, we used a post hoc pairwise *t* test to identify 36 proteins that were significantly overrepresented in one group over the others. Proteins were considered to be increased in abundance by a specific ligand if *p* values in a post hoc *t* test were less than 0.05 for all pairwise tests for that ligand (Table I and supplemental Table S3).

ATP-dependent Interactions—We hypothesized that the use of the ATP hydrolysis-deficient E47A mutant would increase the strength of interaction between HSP90 and ATP-dependent interacting proteins as has been observed previously with the homologous yeast HSP90 (HSC82p) E33A mutant (40). Under this assumption, we expected that proteins identified in the E47A ATP group would also be represented in the WT ATP group at a lower abundance because of the ability of wild type HSP90 to hydrolyze ATP. Consistent with this concept, we found that 26 proteins identified in the E47A ATP complexes were also present in the WT ATP complexes, eight of which were identified at lower abundances in the WT ATP complexes (Fig. 1; FKBP5, SUGT1, AHSA1, NUDCD3, PTGES3 (p23), CSNK1A1, UNC45A, and FAM83H; *t* test *p* value <0.02). These results are consistent with previous findings showing p23 and AHSA1 to have an increased binding affinity for HSP90 in its ATP-bound state (13, 40) and suggest that other interactions in this category may also be positively regulated by ATP.

Geldanamycin-dependent Interactions—Most evidence supports the hypothesis that pharmacological inhibition of HSP90 disrupts its interactions with client proteins and co-chaperones such as p23. Indeed, in several cases, we show that known and novel HSP90 interacting proteins identified in reactions containing ATP are either entirely excluded from HSP90 complexes treated with geldanamycin or are severely reduced in abundance (Fig. 1). However, we also identified 15 HSP90 interactions that are specifically induced after treatment with geldanamycin (*t* test *p* value <0.05). Interestingly, these complexes are enriched for proteins known to function in basic processes of RNA metabolism including POLR2E (RNA polymerase II subunit), C19orf2 (a transcriptional co-repressor known to associate with POLR2E (46, 47)), ASCC3L1 (RNA helicase), RPAP3 and PIH1D1 (ribonucleoprotein assembly factors) (48), and YTHDC2 (putative RNA helicase/splicing factor).

It is well established that HSP70 expression is dramatically up-regulated after treatment with HSP90 inhibitors. As several proteins indentified in geldanamycin-dependent complexes are known to be involved in stress responses, we considered the possibility that these interactors may be likewise up-regulated. We were interested in whether the observed over-abundance in complexes treated with geldanamycin may be a result of increased total cellular protein rather than a direct effect of geldanamycin acting on HSP90. We tested this possibility by determining whether a subset of geldanamycin-dependent interactors were up-regulated using real time RT-PCR. Of the eight proteins tested, only HSP70 homologs HSPA1A and HSPA8 were up-regulated after geldanamycin treatment (supplemental Fig. S7). It is therefore unlikely that the observed increase of these proteins in HSP90 complexes is due to increased cellular abundance. Furthermore, if the binding interaction between HSP90 and HSP70 was only influenced by cellular abundance of these proteins, then we would expect that any increase in HSP70 mRNA expression after GA treatment would be directly reflected in the peptide spectra count. We found that the mRNA abundances for the HSP70 homologs HSPA8 and HSPA1A are 2- and 18-fold up-regulated, respectively, after GA treatment, whereas the spectral abundances for the corresponding proteins were not found to be statistically different (see supplemental Fig. S8; *t* test $p = 0.31$).

As a control, we went further to test the inactive HSP90 ATPase mutant D93N to determine whether the presence of geldanamycin-dependent interactors in HSP90 complexes depended upon an active HSP90 ATPase or the ability of HSP90 to bind nucleotides or geldanamycin (49). The D93N mutation prevents nucleotide binding in the HSP90 ATPase active site and is also predicted to perturb geldanamycin binding based upon the observation that D93N makes contacts with both GA and adenine nucleotides through a similar mechanism (50). We also tested a mutant lacking the C-terminal MEEVD motif (ΔMEEVD), which is known to bind

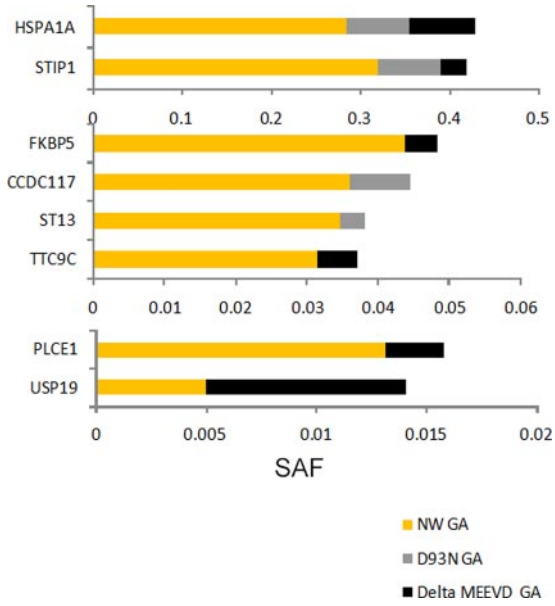

FIG. 2. **Mutations affecting nucleotide binding and TPR domain interactions diminish the effects of geldanamycin on HSP90 complexes.** SAF values for all proteins indentified in purifications containing geldanamycin using N-terminal TAP-tagged HSP90 WT (*yellow*) and/or D93N (*gray*) and ΔMEEVD mutants (*black*) are shown. Proteins that did not pass the filtering criteria in either of the two mutant experimental groups are not shown. All data are averages from three replicate experiments. All statistical data including raw data and standard deviations are available in supplemental Table S1.

HSP90 interactors containing TPR motifs (51–53). We reasoned that interactions with geldanamycin-dependent complex members that contained TPR motifs, such as RPAP3, would be significantly impaired. We stably expressed N-terminally TAP-tagged HSP90 mutants in HEK293T cells, repeated the purifications in the presence of geldanamycin, and compared the results with our original data set. We found that the abundance of the geldanamycin-dependent HSP90 interactors identified in the WT GA group was severely decreased or absent in all cases. Fig. 2 shows the average SAF for all proteins identified in geldanamycin-dependent complexes that were also identified with the D93N or ΔMEEVD mutants. One notable exception was the CS domain-containing protein USP19, which was increased slightly in the ΔMEEVD purifications (*t* test $p = 0.0335$). However, USP19 did not bind the D93N mutant, which is in accordance with the prediction that this CS domain-containing co-chaperone is predicted to bind the N-terminal ATPase domain (45). These results suggest that the effects of geldanamycin on HSP90 complexes are intrinsic to HSP90 and are dependent upon a full ATPase activity and/or the C-terminal MEEVD motif.

CHORDC1 Forms an ADP-dependent Interaction with HSP90—Using the data from the N-terminal TAP-tagged HSP90, we identified c10orf137 (EDRF1) and the CS domain-containing protein CHORDC1 as ADP-regulated HSP90 inter-

actors (*t* test $p < 0.0116$ and 5.0×10^{-8}, respectively). We were intrigued that ADP stimulated the interaction between HSP90 and CHORDC1 when other CS domain-containing family members in our data set appear to bind the ATP-bound HSP90 (PTGES3 (p23), SUGT1, CACYBP, NUDC, and NUDCD3). It is well established that the binding of ATP and ADP to the N-terminal ATPase domain of HSP90 induces conformational changes that influence the client protein and co-chaperone constituents of HSP90 complexes (7, 18–20). The CHORD domain in CHORDC1, like other CS domain-containing proteins, has been shown to interact with the N-terminal ATPase domain of HSP90; however, the role of nucleotide binding in the interaction between HSP90 and CHORDC1 has not been clearly demonstrated (42, 45, 55). It is important to note that slightly more CHORDC1 peptides were identified in the MS/MS analysis of wild type N-TAP complexes *versus* the E74A mutant (Fig. 1*a*, compare NW ATP with NE ATP); however, this apparent increase was not found to be significant (*t* test $p = 0.055$). Furthermore, we were unable to identify CHORDC1 as an ADP-dependent interactor in our MS/MS experiments using the C-terminal TAP-tagged HSP90. Only a single peptide was identified in each of the CE ATP replicates, and no CHORDC1 peptides were observed in the CW ADP group. We attribute this to the generalized capture inefficiency observed for the C-terminal TAP-tagged constructs. Despite this discrepancy, we were interested to verify and further investigate the basis for this observed ADP-dependent interaction.

To verify any effect of the position of the TAP tag and more clearly understand the effects of nucleotides on this interaction, we used a C-terminal TAP-tagged HSP90 and an N-terminal HA-tagged CHORDC1 (HA-CHORDC1) for co-affinity precipitation experiments in the presence of varying ratios of nucleotides. We tested whether the ADP:ATP ratio, and not solely the lack of ATP, was governing the CHORDC1-HSP90 interaction. Co-expressing HEK293T cells were harvested directly into TAP lysis buffer containing either increasing amounts of ADP or decreasing ratios of ADP:ATP by holding the concentration of ADP constant. TAP-tagged HSP90 was then affinity-precipitated with streptavidin beads and washed with lysis buffer containing the appropriate nucleotide ratios, and the bound proteins were eluted and Western blotted. Empty vector constructs (VO) were used to control for non-specific binding. Fig. 3*a* clearly shows that an ADP-dependent interaction with CHORDC1 persists when the C-terminally TAP-tagged HSP90 is used, suggesting that the position of the tag has no effect on the interaction. The 37-kDa HA-CHORDC1 band became visible when ADP alone was added at a concentration as low as 1 μM and reached a maximal intensity at 1 mM (Fig. 3*a*, *upper panel*, *lanes 3–7*). Importantly, no interaction was detected where ADP was not added, suggesting that this interaction was not occurring because the lysates were lacking ATP (Fig. 3*a*, *lanes 2* and *13*). ATP was then titrated into the lysis buffer while holding the ADP concentration constant at the subsaturating concentration of 100 μM. The addition of ATP began to disrupt the interaction at 1 μM. At 100 μM ATP (1:1 ADP:ATP ratio), the interaction was completely abolished, demonstrating an inhibitory effect of ATP on the stability of this complex (Fig. 3*a*, *lanes 8–13*). Densitometry was then performed to quantify the Western blot signal (Fig. 3*a*, *bottom*). To further verify that the position of the TAP tag had no bearing on the interaction, affinity precipitations of HA-CHORDC1 were performed with N-terminal HSP90 TAP-tagged constructs in the presence of 5 mM ATP or 5 mM ADP. In all cases, the 37-kDa HA-CHORDC1 band was clearly visible only in reactions containing ADP (data not shown). Despite the fact that we did not identify CHORDC1 as an ADP-dependent interactor in the MS/MS analysis of affinity precipitations from cells stably expressing the C-terminal TAP-tagged HSP90 (Fig. 1), we clearly demonstrated this interaction in these experiments using transient transfections and Western blotting.

Role of Nucleotide Binding in the ADP-dependent HSP90-CHORDC1 Interaction—Because our results show that high ADP:ATP ratios are stimulating the HSP90-CHORDC1 interaction, we wanted to determine which structural elements of HSP90 are specifically responsible for this activity. We tested 1) whether the HSP90 N-terminus where the ATPase domain resides is sufficient to form the ADP-dependent CHORDC1-HSP90 interaction, 2) whether the nucleotide binding activity of HSP90 is necessary for this interaction, and 3) whether the ATPase activity of HSP90 is essential for the stimulatory activity of ADP. To this end, we co-expressed and affinity-precipitated wild type HA-CHORDC1 with a panel of C-terminal TAP-tagged HSP90 mutants consisting of the isolated N-terminal ATPase domain (HSP90-N), a mutant lacking both nucleotide binding and hydrolysis activities (HSP90 D93N) (49), or a point mutant that lacks ATP hydrolysis activity but retains wild type nucleotide binding activity (HSP90 E47A) (15, 17, 39) (Fig. 3*b*). An attempt was made to construct an HSP90 mutant with the ATPase domain deleted; however, this construct was not tested because of an undetectable level of expression. Affinity precipitation reactions were performed in lysis buffer containing either 1 mM ATP or 1 mM ADP.

The HSP90 E47A mutant precipitated more CHORDC1 than the full-length wild type protein in the reactions containing either ADP or ATP (Fig. 3*c*, compare *lanes 1* and *2* with *lanes 3* and *4*); however, the interaction continued to be specifically stimulated by ADP as was shown for the wild type HSP90. Notably, the HSP90 D93N mutant failed to interact with CHORDC1 in either the ATP or ADP reaction despite robust protein expression. This suggests that CHORDC1 is unable to bind the apoenzyme form of HSP90 and that nucleotide binding is necessary for this interaction. The isolated ATPase domain of HSP90 (HSP90-N) interacted with CHORDC1 in both ATP and ADP reactions, yet the interaction remained positively influenced by ADP. Compared with full-length wild type HSP90, however, the ATPase domain alone appeared to

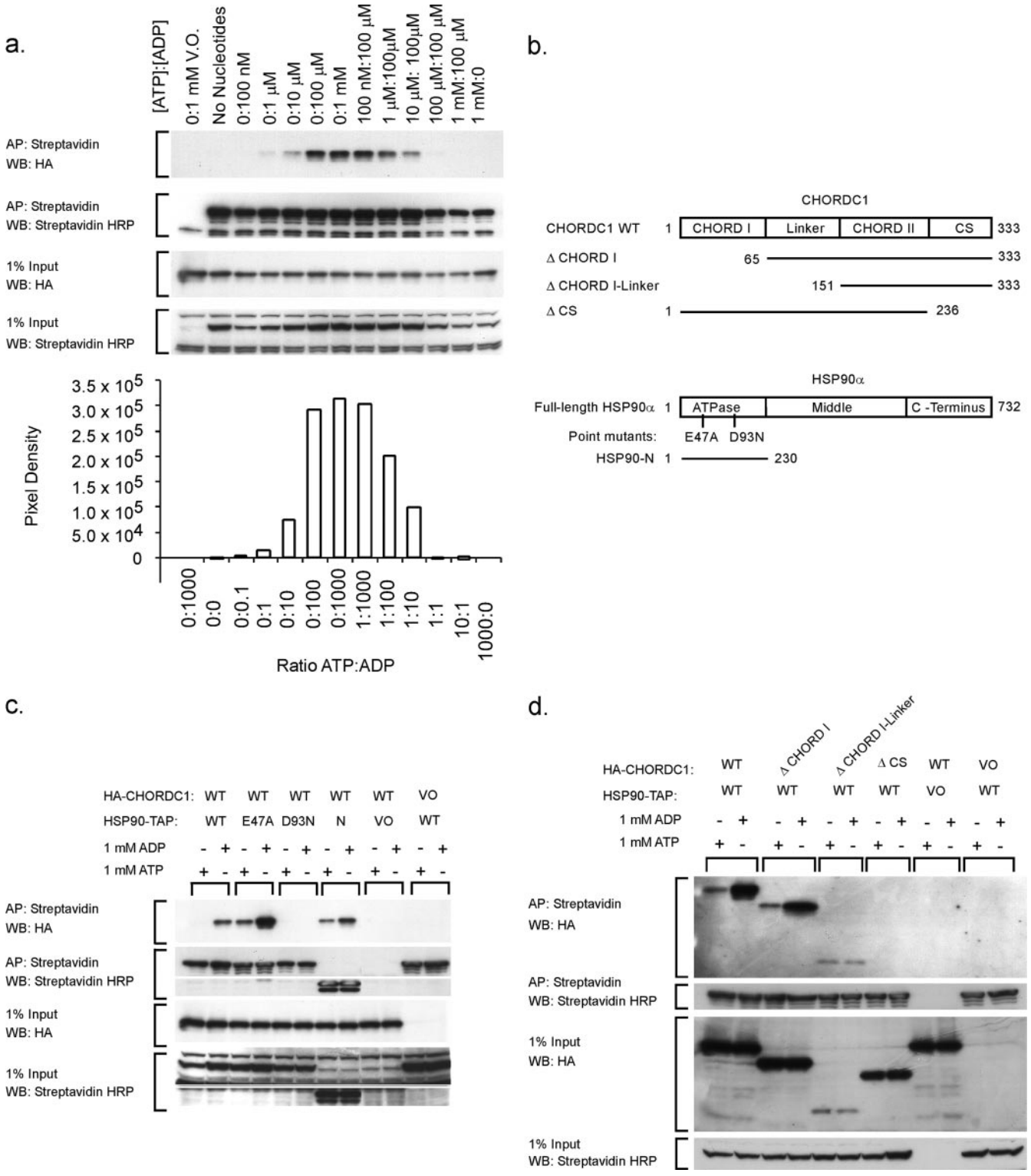

FIG. 3. **HSP90-CHORDC1 interaction is stimulated by high ADP:ATP ratios and is dependent upon elements within HSP90 and CHORDC1.** *a*, Western blot (*WB*) of affinity-precipitated C-terminally TAP-tagged HSP90-CHORDC1 complexes in the presence of increasing amounts of ADP and decreasing ratios of ADP:ATP. Complexes were precipitated with streptavidin beads, washed, and subjected to SDS-PAGE. Blots were probed with streptavidin-horseradish peroxidase (*HRP*) (TAP-HSP90) and anti-HA antibodies (HA-CHORDC1). Vector only (VO) controls are shown in the *lanes* to the *left*, and loading controls are shown in the *two panels below*. Densitometry was used to quantify the CHORDC1 signal for the indicated ATP:ADP ratios. *b*, a schematic diagram of HSP90 and CHORDC1 truncation and point mutants used in this analysis. *Numbers* indicate the amino acid residues. *c*, Western blot of HA-tagged full-length CHORDC1 affinity-precipitated with the

interact with less specificity for ADP as evidenced by the CHORDC1 band appearing in the ATP-containing reaction (Fig. 3*c*, compare *lanes 1* and *2* with *lanes 7* and *8*). This suggests that elements outside the ATPase domain may reinforce the selectivity for this ADP-dependent interaction.

The CHORDC1 protein is composed of two tandem zinc-binding CHORD domains separated by a 90-amino acid linker region and a C-terminal CS domain homologous to the HSP90 binding domain of p23 and SUGT1 (54). Previous studies have shown subsections of the CHORD domain to be essential for CHORDC1 binding to HSP90 in yeast two-hybrid assays (42, 55). Specifically, the N-terminal CHORD domain (CHORDI) was shown to be dispensable for HSP90 binding; however, the linker region and the C-terminal CHORD domain (CHORDII) were shown to be necessary for the full binding interaction. We wanted to determine which elements of CHORDC1 were involved in producing this ADP-dependent interaction with HSP90 and whether deletion of a particular domain would destroy selectivity for ADP. We created N-terminal HA-tagged truncation mutants of CHORDC1 either by deleting the first CHORD domain (ΔCHORDI), deleting CHORDI along with the intervening linker region (ΔCHORDI-Linker), or deleting the C-terminal CS domain (ΔCS) (Fig. 3*b*). We also attempted to test the binding of a CHORDC1 mutant consisting of only the C-terminal CS domain, but this construct failed to be expressed (data not shown). As before, we co-expressed these constructs with C-terminally TAP-tagged wild type full-length HSP90 in HEK293T cells and performed affinity precipitations and Western blots on lysates containing either 1 mM ATP or 1 mM ADP (Fig. 3*d*).

Deletion of the CHORDI domain had no effect on either HSP90 binding or nucleotide selectivity. The amount of ΔCHORDI precipitating with HSP90 was equivalent to the full-length protein, suggesting that the CHORDI domain is dispensable for both HSP90 binding and ADP selectivity. These findings are in agreement with previous two-hybrid studies showing CHORDI to be dispensable for this interaction (42). Interestingly, deletion of the linker region in addition to the CHORDI domain caused the loss of selectivity for ADP. Despite lower protein expression, both ATP and ADP reactions precipitated equivalent amounts of CHORDC1 (Fig. 3d, *lanes 5* and *6*). This raises the possibility that the linker region may play a role in conferring nucleotide selectivity to the CHORDC1-HSP90 interaction. Deletion of the CS domain, however, completely abolished the interaction regardless of nucleotide composition of the reaction (Fig. 3*d*, *lanes 7* and *8*). This result is also in agreement with previous yeast two-hybrid data showing the CS domain to be necessary for HSP90 interactions (42).

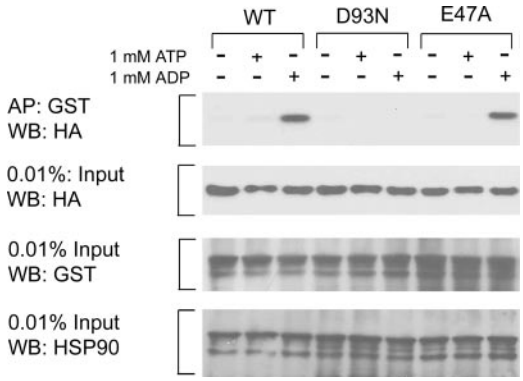

FIG. 4. **CHORDC1 interacts with HSP90 *in vitro* in an ADP-dependent manner.** 1 μg of purified HSP90-GST WT, D93N, and E47A fusions immobilized on glutathione beads was incubated with 100 ng of HA-CHORDC1 for 5 h at 4 °C in the presence of 5 mM ATP or ADP or no nucleotides. Complexes were washed, subjected to SDS-PAGE, and immunoblotted with either anti-HA, anti-GST, or anti-HSP90 antibodies. The double band for HSP90 in the anti-GST and anti-HSP90 immunoblots represents a breakdown product of HSP90. *AP*, affinity precipitation; *WB*, Western blot.

HSP90 and CHORDC1 Interact in an ADP-dependent Manner in Vitro—We went further to confirm whether this ADP-dependent interaction was direct and did not require the presence or activity of additional proteins by performing *in vitro* binding assays using purified recombinant HSP90 and CHORDC1. cDNAs for HA-CHORDC1 and HSP90 (WT, D93N, and E47A) were N-terminally tagged with polyhistidine and GST, respectively; expressed in *E. coli*; and purified. HSP90-GST remained immobilized on glutathione beads throughout the purification procedure, and the beads were then used to affinity precipitate HSP90-CHORDC1 complexes in the presence of ATP and ADP (Fig. 4). As in the co-expression experiments presented above, recombinant CHORDC1 binding to WT and E47A HSP90 was greatly increased only in the presence of 1 mM ADP, whereas no binding was detected with HSP90 D93N regardless of the nucleotide present in the reaction.

DISCUSSION

HSP90 Interactome Is Dynamic with Respect to Nucleotides and Geldanamycin—Several recent studies presented profiles of the human HSP90 interactome using immunopurifications and affinity capture with immobilized HSP90 (23, 27). These studies effectively identified several new and novel HSP90 interactors; however, these experiments were not designed to identify interactions that are sensitive to HSP90 ligands. In addition to presenting evidence for 24 novel HSP90-interacting proteins, we have gone further to identify 52 proteins (84%

indicated C-terminally TAP-tagged HSP90α mutants in the presence of 1 mM ATP or 1 mM ADP. Complexes were purified and probed as in *a*. Vector only controls are shown in the *two lanes* to the *extreme right*. *d*, Western blot of HA-tagged CHORDC1 truncation mutants affinity-precipitated with TAP-tagged full-length wild type HSP90α in the presence of 1 mM ATP and 1 mM ADP and probed as in *a*. Vector only controls are shown in the *two lanes* to the *extreme right*. *AP*, affinity precipitation.

of total identifications) that interacted with HSP90 in a ligand-dependent manner (ANOVA $p < 0.01$), 43 of which (HSP70 homologs included) were significantly overrepresented in one ligand group over the others, presenting evidence that these interactions hold specificity for a particular ligand-bound form of HSP90 (Table I). These findings suggest that the HSP90 interactome is strongly influenced by nucleotide and drug ligands. Of these regulated interactions, approximately half were overrepresented in complexes containing the HSP90α E47A mutant. Because this mutant binds but does not hydrolyze ATP, we predict that proteins identified with this mutant are either completely ATP-dependent or at least in some cases positively influenced by ATP binding. To date, our TAP method utilizing the E47A mutant has yielded the largest number of identifications of known HSP90 interacting co-chaperones. Most notably, we have identified seven members of the CS domain-containing co-chaperone family, including two novel interactions (USP19 and NUDCD3). This is the most complete representation of this family of HSP90 interactors presented thus far and demonstrates the ability of this technique to identify known and novel HSP90 interactions. Despite the presence of 5 mM ATP and an ATP regeneration system, the WT ATP purifications appeared to produce significantly fewer interactions than the E47A mutant. This was not entirely unexpected as it has been previously shown that interactions with the wild type HSP90 are relatively transient (17). Interestingly, we identified PLCE1 (phospholipase C type E1) as a protein that binds abundantly to WT HSP90 regardless of the ligand present in the purifications but that was not detectible in reactions containing the E47A mutant. We cannot eliminate the possibility that clonal effects may have some influence or that structural effects of the E47A mutation somehow exclude this interaction; however, the significant number of known HSP90 interactors identified with the E47A mutant suggests that clonal effects are minimal.

Geldanamycin-dependent HSP90 Complexes Are Enriched for Core Transcription Machinery—The majority of interaction studies focused on HSP90 client proteins show that pharmacological inhibition of ATPase activity leads to disruption of HSP90 complexes. Indeed, we show that most interactions that were shown to be ATP-dependent are in fact disrupted by geldanamycin treatment. Interestingly, we identified several HSP90 interactions that appear to be reinforced by geldanamycin treatment. Several proteins in these geldanamycin-dependent complexes, including HSP70, RPAP3, c19orf2, PIH1D1, and EFTUD2, were also reported in a proteomics study as interacting with core transcription machinery (57). The concordance between these two studies suggests the interesting possibility that HSP90 is involved in regulating transcription at several levels and that the activity of geldanamycin may alter fundamental transcriptional processes.

The HSP90 interactor RPAP3 makes five interactions with components of core transcription machinery identified in geldanamycin-dependent complexes (c19orf2, POLR2E, EFTUD2, HSP70, and PIH1D1), suggesting that this protein may serve as a bridge for an HSP90 subcomplex. RPAP3 contains two TPR domains that have been shown in other proteins to bind the C-terminal MEEVD motif on HSP90 and HSP70. It is possible that this interaction is also mediated by the MEEVD motif on the C terminus of HSP90 because RPAP3 was absent in our MS/MS analysis of HSP90 ΔMEEVD mutant complexes (supplemental Table S3). In support of this notion, RPAP3 (hSpagh) was first identified as an HSP90-interacting protein using the isolated C-terminal domain, suggesting that this protein binds the HSP90 C terminus (23), and was recently shown to bind HSP90 directly and function in a small nucleolar ribonucleoprotein assembly complex containing HSP90, PIH1D1, RUVBL1, and RUVBL2 (48). Notably, RUVBL1 and RUVBL2 were also identified as components of geldanamycin-dependent complexes in our experiments; however, these proteins were present in our empty vector control (VO ATP) purifications and were consequently filtered (data not shown). In this case, it is unlikely that RPAP3 and PIH1D1 are contaminants being carried nonspecifically because both of these proteins are entirely absent in all groups except for the vector control and those treated with geldanamycin, and the quantity of the RUVBL1/2 proteins does not increase concordantly with PIH1D1 and RPAP3 in the geldanamycin-dependent complexes.

HSP70 (HSPA1A) is one of the most abundant proteins among the geldanamycin-dependent complexes and is known to interact with four other proteins identified in these complexes including STIP1 (HOP). It is well established that HSP70 homologs interact with HSP90 through binding to STIP1, and this suggests that STIP1 may act as an adaptor protein in our experiments (58, 59). However, this interaction was not stimulated by geldanamycin treatment in our experiments, suggesting that the interaction between HSP70 and HSP90 may either be independent of HOP or that geldanamycin treatment may fortify the interaction between an existing HSP90-HOP complex and HSP70.

CHORDC1 Interaction Is Stimulated by ADP—We have identified and characterized CHORDC1 as an ADP-dependent HSP90-interacting protein. We further show that high ADP:ATP ratios stimulate binding and that this selectivity can be traced to elements within the linker region residing between the two tandem CHORD domains. Certain lines of evidence suggest that this interaction is direct. First, we were unable to detect other proteins with increases in SAF values proportional to CHORDC1 for purifications containing ADP in our MS experiments that would indicate a cofactor or adaptor protein (Fig. 1 and supplemental Table S3). Second, the heterologously expressed purified recombinant proteins interact *in vitro* in an ADP-dependent manner (Fig. 4). These results taken together with the fact that the CS domain has been shown in several proteins to be a direct HSP90 binding element (3, 23, 42–44) lead us to propose the possibility that this interaction is direct.

Our results are generally in agreement with those presented by Wu *et al.* (42) showing that the interaction between HSP90 and CHORDC1 (Chp1) is independent of ATP. Indeed, we did observe a low affinity interaction in the presence of ATP (Fig. 3d, *lane 1*). We believe this to be the low affinity, nucleotide-independent interaction reported previously. Importantly, this group did not report experiments testing the effects of ADP on this complex, so to our knowledge, our results are the first to demonstrate the effects of ADP on this interaction.

Melusin (ITGB1BP2), a homolog of CHORDC1, is the only other CHORD domain-containing protein in the human proteome and has been shown to interact with HSP90 (56). We predicted that this protein, like CHORDC1, would bind HSP90 in an ADP-dependent manner. In co-expression experiments and *in vitro* with purified proteins, we were indeed able to detect an ADP-dependent HSP90 interaction with melusin; however, this was only observed with the HSP90 E47A mutant, and no significant increase in binding was observed with the wild type HSP90 and ADP (data not shown). Melusin and CHORDC1 show homology within the CHORD domains; however, they are only 42% identical in the region containing the 90-amino acid linker and the CHORDII domain (BlastP, NCBI) that we have shown to modulate the ADP-dependent interaction between HSP90 and CHORDC1. It is therefore possible that this sequence diversity could lead to altered HSP90 binding activity. Furthermore, the relative binding affinities of ADP for wild type HSP90 and the E47A mutant have not been determined. It is therefore possible that this mutant binds ADP more tightly than the wild type protein, thus contributing to the increased effect of ADP in the melusin-HSP90 interaction. In support of this notion, we have also observed increased CHORDC1 binding to the E47A mutant relative to WT HSP90 in the presence of ADP in co-expression experiments (Fig. 3*c*, compare *lanes 1* and *2* with *lanes 3* and *4*), which suggests that the E47A mutation positively affects the ADP-dependent interaction with CHORDC1 and that this phenomenon may therefore be extended to melusin. However, the E47A mutant bound similar amounts of HA-CHORDC1 in the presence of ADP in the *in vitro* binding assays (Fig. 4). This may be due to a slightly higher expression of the E47A mutant in the co-expression experiments that was not detected in our Western blots (see Fig. 3).

The observation that CHORDC1 is stimulated to bind HSP90 when the ATP:ADP ratio falls below 1 raises the possibility that the HSP90-CHORDC1 interaction may be involved in the response to altered energy balance *in vivo*. The ADP:ATP ratio has been shown to exceed 1 under conditions of oxidative stress combined with a glycolytic blockade (60). Furthermore, melusin has been shown to be required for recovery from dilated cardiomyopathy, which is marked by acute depletion of ATP and an increase in the ADP:ATP ratio (56, 61–63). This suggests a possible role for the CHORD domain in response to metabolic stress. It remains to be tested whether the HSP90-CHORDC1 interaction can be observed in living cells under conditions that permit ATP depletion. These experiments may further develop our understanding of the function of the CHORD domain in stress responses.

Acknowledgments—We thank the Clinical Division at the Fred Hutchinson Cancer Research Center for supporting this research. We also thank Eric Foss, Phil Gafken, Jason Hogan, and Tomoko Hamma at the Fred Hutchinson Cancer Research Center for critical input and technical support.

* This work was supported, in whole or in part, by the National Institutes of Health through Public Health Service, National Research Service Award T32 GM07270 from the NIGMS and the Clinical Research Division at the Fred Hutchinson Cancer Research Center.

S The on-line version of this article (available at http://www.mcponline.org) contains supplemental Figures and Tables S1–S9.

¶ To whom correspondence should be addressed: Fred Hutchinson Cancer Research Center, D2-100, P. O. Box 19024, Seattle, WA 98109. Tel.: 206-667-6241; Fax: 206-667-5255; E-mail: jsimon@fhcrc.org.

REFERENCES

1. Powers, M. V., and Workman, P. (2006) Targeting of multiple signalling pathways by heat shock protein 90 molecular chaperone inhibitors. *Endocr.-Relat. Cancer* **13,** Suppl. 1, S125–S135
2. Pearl, L. H., and Prodromou, C. (2006) Structure and mechanism of the Hsp90 molecular chaperone machinery. *Annu. Rev. Biochem.* **75,** 271–294
3. Lee, Y. T., Jacob, J., Michowski, W., Nowotny, M., Kuznicki, J., and Chazin, W. J. (2004). Human Sgt1 binds HSP90 through the CHORD-Sgt1 domain and not the tetratricopeptide repeat domain. *J. Biol. Chem.* **279,** 16511–16517
4. Riggs, D. L., Cox, M. B., Cheung-Flynn, J., Prapapanich, V., Carrigan, P. E., and Smith, D. F. (2004) Functional specificity of co-chaperone interactions with Hsp90 client proteins. *Crit. Rev. Biochem. Mol. Biol.* **39,** 279–295
5. Pearl, L. H. (2005) Hsp90 and Cdc37—a chaperone cancer conspiracy. *Curr. Opin. Genet. Dev.* **15,** 55–61
6. Roe, S. M., Ali, M. M., Meyer, P., Vaughan, C. K., Panaretou, B., Piper, P. W., Prodromou, C., and Pearl, L. H. (2004) The mechanism of Hsp90 regulation by the protein kinase-specific cochaperone p50(cdc37). *Cell* **116,** 87–98
7. Siligardi, G., Hu, B., Panaretou, B., Piper, P. W., Pearl, L. H., and Prodromou, C. (2004) Co-chaperone regulation of conformational switching in the Hsp90 ATPase cycle. *J. Biol. Chem.* **279,** 51989–51998
8. Colombo, G., Morra, G., Meli, M., and Verkhivker, G. (2008) Understanding ligand-based modulation of the Hsp90 molecular chaperone dynamics at atomic resolution. *Proc. Natl. Acad. Sci. U.S.A.* **105,** 7976–7981
9. Meyer, P., Prodromou, C., Liao, C., Hu, B., Mark Roe, S., Vaughan, C. K., Vlasic, I., Panaretou, B., Piper, P. W., and Pearl, L. H. (2004) Structural basis for recruitment of the ATPase activator Aha1 to the Hsp90 chaperone machinery. *EMBO J.* **23,** 511–519
10. Lotz, G. P., Lin, H., Harst, A., and Obermann, W. M. (2003) Aha1 binds to the middle domain of Hsp90, contributes to client protein activation, and stimulates the ATPase activity of the molecular chaperone. *J. Biol. Chem.* **278,** 17228–17235
11. Panaretou, B., Siligardi, G., Meyer, P., Maloney, A., Sullivan, J. K., Singh, S., Millson, S. H., Clarke, P. A., Naaby-Hansen, S., Stein, R., Cramer, R., Mollapour, M., Workman, P., Piper, P. W., Pearl, L. H., and Prodromou, C. (2002) Activation of the ATPase activity of hsp90 by the stress-regulated cochaperone aha1. *Mol. Cell* **10,** 1307–1318
12. Harst, A., Lin, H., and Obermann, W. M. (2005) Aha1 competes with Hop, p50 and p23 for binding to the molecular chaperone Hsp90 and contributes to kinase and hormone receptor activation. *Biochem. J.* **387,** 789–796
13. McLaughlin, S. H., Sobott, F., Yao, Z. P., Zhang, W., Nielsen, P. R., Grossmann, J. G., Laue, E. D., Robinson, C. V., and Jackson, S. E. (2006) The co-chaperone p23 arrests the Hsp90 ATPase cycle to trap client proteins. *J. Mol. Biol.* **356,** 746–758

14. Sullivan, W. P., Owen, B. A., and Toft, D. O. (2002) The influence of ATP and p23 on the conformation of hsp90. *J. Biol. Chem.* **277,** 45942–45948
15. Obermann, W. M., Sondermann, H., Russo, A. A., Pavletich, N. P., and Hartl, F. U. (1998) In vivo function of Hsp90 is dependent on ATP binding and ATP hydrolysis. *J. Cell Biol.* **143,** 901–910
16. Whitesell, L., and Cook, P. (1996) Stable and specific binding of heat shock protein 90 by geldanamycin disrupts glucocorticoid receptor function in intact cells. *Mol. Endocrinol.* **10,** 705–712
17. Young, J. C., and Hartl, F. U. (2000) Polypeptide release by Hsp90 involves ATP hydrolysis and is enhanced by the co-chaperone p23. *EMBO J.* **19,** 5930–5940
18. Shiau, A. K., Harris, S. F., Southworth, D. R., and Agard, D. A. (2006) Structural Analysis of E. coli hsp90 reveals dramatic nucleotide-dependent conformational rearrangements. *Cell* **127,** 329–340
19. Krukenberg, K. A., Förster, F., Rice, L. M., Sali, A., and Agard, D. A. (2008) Multiple conformations of E. coli Hsp90 in solution: insights into the conformational dynamics of Hsp90. *Structure* **16,** 755–765
20. Morra, G., Verkhivker, G., and Colombo, G. (2009) Modeling signal propagation mechanisms and ligand-based conformational dynamics of the Hsp90 molecular chaperone full-length dimer. *PLoS Comput. Biol.* **5,** e1000323
21. Zhao, R., Davey, M., Hsu, Y. C., Kaplanek, P., Tong, A., Parsons, A. B., Krogan, N., Cagney, G., Mai, D., Greenblatt, J., Boone, C., Emili, A., and Houry, W. A. (2005) Navigating the chaperone network: an integrative map of physical and genetic interactions mediated by the hsp90 chaperone. *Cell* **120,** 715–727
22. Falsone, S. F., Gesslbauer, B., Tirk, F., Piccinini, A. M., and Kungl, A. J. (2005) A proteomic snapshot of the human heat shock protein 90 interactome. *FEBS Lett.* **579,** 6350–6354
23. Te, J., Jia, L., Rogers, J., Miller, A., and Hartson, S. D. (2007) Novel subunits of the mammalian Hsp90 signal transduction chaperone. *J. Proteome Res.* **6,** 1963–1973
24. Falsone, S. F., Gesslbauer, B., Rek, A., and Kungl, A. J. (2007) A proteomic approach towards the Hsp90-dependent ubiquitinylated proteome. *Proteomics* **7,** 2375–2383
25. Schumacher, J. A., Crockett, D. K., Elenitoba-Johnson, K. S., and Lim, M. S. (2007) Proteome-wide changes induced by the Hsp90 inhibitor, geldanamycin in anaplastic large cell lymphoma cells. *Proteomics* **7,** 2603–2616
26. Maloney, A., Clarke, P. A., Naaby-Hansen, S., Stein, R., Koopman, J. O., Akpan, A., Yang, A., Zvelebil, M., Cramer, R., Stimson, L., Aherne, W., Banerji, U., Judson, I., Sharp, S., Powers, M., deBilly, E., Salmons, J., Walton, M., Burlingame, A., Waterfield, M., and Workman, P. (2007) Gene and protein expression profiling of human ovarian cancer cells treated with the heat shock protein 90 inhibitor 17-allylamino-17-demethoxygeldanamycin. *Cancer Res.* **67,** 3239–3253
27. Tsaytler, P. A., Krijgsveld, J., Goerdayal, S. S., Rüdiger, S., and Egmond, M. R. (2009) Novel Hsp90 partners discovered using complementary proteomic approaches. *Cell Stress Chaperones* **14,** 629–638
28. Angers, S., Thorpe, C. J., Biechele, T. L., Goldenberg, S. J., Zheng, N., MacCoss, M. J., and Moon, R. T. (2006) The KLHL12-Cullin-3 ubiquitin ligase negatively regulates the Wnt-beta-catenin pathway by targeting Dishevelled for degradation. *Nat. Cell Biol.* **8,** 348–357
29. Hutchison, K. A., Czar, M. J., Scherrer, L. C., and Pratt, W. B. (1992) Monovalent cation selectivity for ATP-dependent association of the glucocorticoid receptor with hsp70 and hsp90. *J. Biol. Chem.* **267,** 14047–14053
30. Motojima, F., and Yoshida, M. (2003) Discrimination of ATP, ADP, and AMPPNP by chaperonin GroEL: hexokinase treatment revealed the exclusive role of ATP. *J. Biol. Chem.* **278,** 26648–26654
31. Chen, G. I., and Gingras, A. C. (2007) Affinity-purification mass spectrometry (AP-MS) of serine/threonine phosphatases. *Methods* **42,** 298–305
32. Craig, R., and Beavis, R. C. (2004) TANDEM: matching proteins with tandem mass spectra. *Bioinformatics* **20,** 1466–1467
33. MacLean, B., Eng, J. K., Beavis, R. C., and McIntosh, M. (2006) General framework for developing and evaluating database scoring algorithms using the TANDEM search engine. *Bioinformatics* **22,** 2830–2832
34. Nesvizhskii, A. I., Keller, A., Kolker, E., and Aebersold, R. (2003) A statistical model for identifying proteins by tandem mass spectrometry. *Anal. Chem.* **75,** 4646–4658
35. Rauch, A., Bellew, M., Eng, J., Fitzgibbon, M., Holzman, T., Hussey, P., Igra, M., Maclean, B., Lin, C. W., Detter, A., Fang, R., Faca, V., Gafken, P., Zhang, H., Whiteaker, J., States, D., Hanash, S., Paulovich, A., and McIntosh, M. W. (2006) Computational Proteomics Analysis System (CPAS): an extensible, open-source analytic system for evaluating and publishing proteomic data and high throughput biological experiments. *J. Proteome Res.* **5,** 112–121
36. Elias, J. E., and Gygi, S. P. (2007) Target-decoy search strategy for increased confidence in large-scale protein identifications by mass spectrometry. *Nat. Methods* **4,** 207–214
37. Florens, L., Carozza, M. J., Swanson, S. K., Fournier, M., Coleman, M. K., Workman, J. L., and Washburn, M. P. (2006) Analyzing chromatin remodeling complexes using shotgun proteomics and normalized spectral abundance factors. *Methods* **40,** 303–311
38. Huang, X., Powell-Coffman, J. A., and Jin, Y. (2004) The AHR-1 aryl hydrocarbon receptor and its co-factor the AHA-1 aryl hydrocarbon receptor nuclear translocator specify GABAergic neuron cell fate in C. elegans. *Development* **131,** 819–828
39. Grenert, J. P., Johnson, B. D., and Toft, D. O. (1999) The importance of ATP binding and hydrolysis by hsp90 in formation and function of protein heterocomplexes. *J. Biol. Chem.* **274,** 17525–17533
40. Millson, S. H., Truman, A. W., King, V., Prodromou, C., Pearl, L. H., and Piper, P. W. (2005) A two-hybrid screen of the yeast proteome for Hsp90 interactors uncovers a novel Hsp90 chaperone requirement in the activity of a stress-activated mitogen-activated protein kinase, Slt2p (Mpk1p). *Eukaryot. Cell* **4,** 849–860
41. Zybailov, B., Coleman, M. K., Florens, L., and Washburn, M. P. (2005) Correlation of relative abundance ratios derived from peptide ion chromatograms and spectrum counting for quantitative proteomic analysis using stable isotope labeling. *Anal. Chem.* **77,** 6218–6224
42. Wu, J., Luo, S., Jiang, H., and Li, H. (2005) Mammalian CHORD-containing protein 1 is a novel heat shock protein 90-interacting protein. *FEBS Lett.* **579,** 421–426
43. Lingelbach, L. B., and Kaplan, K. B. (2004) The interaction between Sgt1p and Skp1p is regulated by HSP90 chaperones and is required for proper CBF3 assembly. *Mol. Cell. Biol.* **24,** 8938–8950
44. Johnson, J. L., and Toft, D. O. (1995) Binding of p23 and hsp90 during assembly with the progesterone receptor. *Mol. Endocrinol.* **9,** 670–678
45. Garcia-Ranea, J. A., Mirey, G., Camonis, J., and Valencia, A. (2002) p23 and HSP20/alpha-crystallin proteins define a conserved sequence domain present in other eukaryotic protein families. *FEBS Lett.* **529,** 162–167
46. Dorjsuren, D., Lin, Y., Wei, W., Yamashita, T., Nomura, T., Hayashi, N., and Murakami, S. RMP, a novel RNA polymerase II subunit 5-interacting protein, counteracts transactivation by hepatitis B virus X protein. *Mol. Cell Biol.* 1998 Dec; 18(12): 7546–55
47. Gstaiger, M., Luke, B., Hess, D., Oakeley, E. J., Wirbelauer, C., Blondel, M., Vigneron, M., Peter, M., and Krek, W. (2003) Control of nutrient-sensitive transcription programs by the unconventional prefoldin URI. *Science* **302,** 1208–1212
48. Boulon, S., Marmier-Gourrier, N., Pradet-Balade, B., Wurth, L., Verheggen, C., Jády, B. E., Rothé, B., Pescia, C., Robert, M. C., Kiss, T., Bardoni, B., Krol, A., Branlant, C., Allmang, C., Bertrand, E., and Charpentier, B. (2008) The Hsp90 chaperone controls the biogenesis of L7Ae RNPs through conserved machinery. *J. Cell Biol.* **180,** 579–595
49. Panaretou, B., Prodromou, C., Roe, S. M., O'Brien, R., Ladbury, J. E., Piper, P. W., and Pearl, L. H. (1998) ATP binding and hydrolysis are essential to the function of the Hsp90 molecular chaperone in vivo. *EMBO J.* **17,** 4829–4836
50. Roe, S. M., Prodromou, C., O'Brien, R., Ladbury, J. E., Piper, P. W., and Pearl, L. H. (1999) Structural basis for inhibition of the Hsp90 molecular chaperone by the antitumor antibiotics radicicol and geldanamycin. *J. Med. Chem.* **42,** 260–266
51. Onuoha, S. C., Coulstock, E. T., Grossmann, J. G., and Jackson, S. E. (2008) Structural studies on the co-chaperone Hop and its complexes with Hsp90. *J. Mol. Biol.* **379,** 732–744
52. Johnson, B. D., Schumacher, R. J., Ross, E. D., and Toft, D. O. (1998) Hop modulates Hsp70/Hsp90 interactions in protein folding. *J. Biol. Chem.* **273,** 3679–3686
53. Richter, K., Muschler, P., Hainzl, O., Reinstein, J., and Buchner, J. (2003) Sti1 is a non-competitive inhibitor of the Hsp90 ATPase. Binding prevents the N-terminal dimerization reaction during the ATPase cycle. *J. Biol. Chem.* **278,** 10328–10333

54. Brancaccio, M., Menini, N., Bongioanni, D., Ferretti, R., De Acetis, M., Silengo, L., and Tarone, G. Chp-1 and melusin, two CHORD containing proteins in vertebrates. FEBS Lett. 2003 Sep 11;551(1–3): 47–52
55. Hahn, J. S. (2005) Regulation of Nod1 by Hsp90 chaperone complex. *FEBS Lett.* **579,** 4513–4519
56. Sbroggiò, M., Ferretti, R., Percivalle, E., Gutkowska, M., Zylicz, A., Michowski, W., Kuznicki, J., Accornero, F., Pacchioni, B., Lanfranchi, G., Hamm, J., Turco, E., Silengo, L., Tarone, G., and Brancaccio, M. (2008) The mammalian CHORD-containing protein melusin is a stress response protein interacting with Hsp90 and Sgt1. *FEBS Lett.* **582,** 1788–1794
57. Jeronimo, C., Forget, D., Bouchard, A., Li, Q., Chua, G., Poitras, C., Thérien, C., Bergeron, D., Bourassa, S., Greenblatt, J., Chabot, B., Poirier, G. G., Hughes, T. R., Blanchette, M., Price, D. H., and Coulombe, B. (2007) Systematic analysis of the protein interaction network for the human transcription machinery reveals the identity of the 7SK capping enzyme. *Mol. Cell* **27,** 262–274
58. Wegele, H., Wandinger, S. K., Schmid, A. B., Reinstein, J., and Buchner, J. (2006) Substrate transfer from the chaperone Hsp70 to Hsp90. *J. Mol. Biol.* **356,** 802–811
59. Wegele, H., Müller, L., and Buchner, J. (2004) Hsp70 and Hsp90—a relay team for protein folding. *Rev. Physiol. Biochem. Pharmacol.* **151,** 1–44
60. Tretter, L., Chinopoulos, C., and Adam-Vizi, V. (1997) Enhanced depolarization-evoked calcium signal and reduced [ATP]/[ADP] ratio are unrelated events induced by oxidative stress in synaptosomes. *J. Neurochem.* **69,** 2529–2537
61. De Acetis, M., Notte, A., Accornero, F., Selvetella, G., Brancaccio, M., Vecchione, C., Sbroggiò, M., Collino, F., Pacchioni, B., Lanfranchi, G., Aretini, A., Ferretti, R., Maffei, A., Altruda, F., Silengo, L., Tarone, G., and Lembo, G. (2005) Cardiac overexpression of melusin protects from dilated cardiomyopathy due to long-standing pressure overload. *Circ. Res.* **96,** 1087–1094
62. Ventura-Clapier, R., Garnier, A., and Veksler, V. (2004) Energy metabolism in heart failure. *J. Physiol.* **555,** 1–13
63. Beer, M., Seyfarth, T., Sandstede, J., Landschütz, W., Lipke, C., Köstler, H., von Kienlin, M., Harre, K., Hahn, D., and Neubauer, S. (2002) Absolute concentrations of high-energy phosphate metabolites in normal, hypertrophied, and failing human myocardium measured noninvasively with (31)P-SLOOP magnetic resonance spectroscopy. *J. Am. Coll. Cardiol.* **40,** 1267–1274